

High resolution spectroscopy over 8500 – 8750 Å for GAIA^{*,**,***}

II. A library of synthetic spectra for $T_{\text{eff}} \leq 7500$ K

U. Munari^{1,2} and F. Castelli³

¹ Osservatorio Astronomico di Padova, Sede di Asiago, I-36012 Asiago (VI), Italy

² Centro Interpardiamentale Studi ed Attività Spaziali (CISAS “G. Colombo”), Università di Padova, Italy

³ CNR-GNA-Osservatorio Astronomico di Trieste Via Tiepolo 11, I-34131 Trieste, Italy

Received September 9; accepted October 4, 1999

Abstract. We present a library of synthetic spectra characterized by $-2.5 \leq [Z/Z_{\odot}] \leq +0.5$, $4.5 \leq \log g \leq 1.0$, and $T_{\text{eff}} \leq 7500$ K computed at the same $\lambda/\Delta\lambda = 20000$ resolving power of the observed spectra given in Paper I for 131 standard stars mapping the MKK spectral classification system. This range of parameters includes the majority of the galactic stars expected to dominate the GAIA target population, i.e. F-G-K-M type stars with metallicity ranging from that of the galactic globular clusters to Population I objects. Extension to $T_{\text{eff}} > 7500$ K will be given later on in this series. The 254 synthetic spectra presented here are based on Kurucz’s codes and line data and have been computed over a more extended wavelength interval (7650 – 8750 Å) than that currently baselined for implementation on GAIA, i.e. the 8500 – 8750 Å. This last range is dominated by the near-IR Ca II triplet and the head of the Paschen series. The more extended wavelength range allows us to investigate the behaviour of other strong near-IR spectral features (severely contaminated by telluric absorptions in ground-based observed spectra) as the K I doublet (7664, 7699 Å), the Na I doublet (8183, 8194 Å) and the lines of Fe I multiplet N.60 at 8327 and 8388 Å. The synthetic spectra support our previous conclusions about the superior performance of the Paschen/Ca II 8500 – 8750 Å region in meeting the GAIA requirements when compared to other near-IR intervals of similar $\Delta\lambda = 250$ Å.

Key words: atlases — surveys — stars: fundamental parameters

1. Introduction

This second paper continues the evaluation study of the expected spectroscopic performances for the GAIA astrometric mission planned by ESA and the establishment of an extensive databank of input data for simulations of GAIA observations. As for the whole series, the results are also of general interest to ground-based spectroscopists working at moderately high resolving powers ($\lambda/\Delta\lambda \sim 10^4$) in the near-IR region of the spectrum.

The astrophysical outlines of the GAIA mission are discussed by Gilmore et al. (1998, and references therein) and an outlook of the GAIA payload and spacecraft is presented by Mérat et al. (1999). The goals of GAIA spectroscopy, the merits of the 8500 – 8750 Å region and a summary of the topics to be addressed in the present series of papers are given in Table 1 of Munari (1999, hereafter M 99).

In Paper I (Munari & Tomasella 1999) we have built up a homogeneous *observational* databank composed by the spectra of 131 standard stars mapping the MKK classification system from types O4 to M 8 and luminosity classes from I to V.

In Paper II we present a library of 254 *synthetic* spectra mapping the part of the $[Z/Z_{\odot}]$, $\log g$ and T_{eff} space where the majority of GAIA targets will be located. The targets are mainly F–G–K–M stars with metallicities ranging from those of the galactic globular clusters to that of the Pop. I objects, thus we computed a grid of synthetic spectra for $-2.5 \leq [Z/Z_{\odot}] \leq +0.5$, $4.5 \leq \log g \leq 1.0$ and $T_{\text{eff}} \leq 7500$ K. Extension to O-B-A stars will be given later

Send offprint requests to: U. Munari, e-mail: munari@pd.astro.it

* Table 2 are only available in electronic form at the CDS via anonymous ftp to cdsarc.u-strasbg.fr (130.79.128.5) or via <http://cdsweb.u-strasbg.fr/Abstract.html>

** Figures 5–93 are only available in electronic form at the <http://www.edpsciences.org>

*** The spectra are also available in electronic form at the CDS or via the personal HomePage <http://ulisse.pd.astro.it/Astro/Atlases/>

on in this series by Castelli & Munari (1999, in preparation). The synthetic spectra match in resolving power the observed ones ($\lambda/\Delta\lambda = 20000$), thus forming an ideal companion set to the data discussed in Paper I.

M 99 outlined the superior merits for implementation on GAIA of the 8500 – 8750 Å region compared to other near-IR wavelength intervals of similar $\Delta\lambda = 250$ Å extension (in the current GAIA baseline configuration the range available for spectroscopy amount to $\Delta\lambda \sim 250$). The near-IR triplet of Ca II and the head of the hydrogen Paschen series lie here. Strong He I and N I lines are found here in early type spectra while in cooler stars lines of Fe I, Si I, Mg I and Ti I are abundant over the 8500 – 8750 Å.

The argument raised by M 99 in support of the 8500 – 8750 Å interval originated both from data from the literature as well as from an extensive and high resolution mapping of the MKK classification scheme from the near-UV to near-IR wavelength domains (Tomasella & Munari, in preparation). However, telluric absorptions dominate over most of the near-IR (cf. Fig. 3 of Paper I), where GAIA is currently baselined to perform the spectroscopic observations. Therefore, a firmer assessment of the capabilities of GAIA spectroscopy from space must be supported by synthetic spectra which can map a finer and more complete grid of parameters than possible with *observed* spectra, without the dramatic contamination by the blocking telluric absorptions.

To this aim the computation of the synthetic spectra was not limited to the 250 Å interval currently baselined for implementation on GAIA (8500 – 8750 Å), but instead expanded to cover the whole 7650 – 8750 Å range, thus including the the K I doublet at 7664, 7699 Å, the Na I doublet at 8183, 8194 Å and the lines of Fe I multiplet 60 at 8327 and 8388 Å. Such K I, Fe I and Na I lines are identified by filled circles in Fig. 1, together with the Ca II triplet at 8498, 8542 and 8662 Å.

We will comment in the last section of this paper how the synthetic spectra presented here support the M 99 conclusions about the superior performance of the 8500 – 8750 Å interval compared to equivalent $\Delta\lambda = 250$ Å centered on the K I, the Fe I or the Na I doublets.

2. The grid of synthetic spectra

The grid of 254 computed spectra is listed in Table 1. The range in temperature extends from 3 500 to 7 500 K, with a 250 K step. The models have been computed for metallicities $[Z/Z_{\odot}] = -2.5, -1.5, -0.5, 0.0$ and $+0.5$. For each $T_{\text{eff}}, [Z/Z_{\odot}]$ pair, three spectra at different surface gravities are given which roughly correspond to luminosity classes V, III, and I in the MKK classification system. The surface gravities are $\log g = 4.5, 2.0$ and 1.0 for $3500 \leq T_{\text{eff}} \text{ (K)} \leq 5 000$, and $\log g = 4.5, 3.0$ and 2.0 for the hotter models. Only the spectrum corresponding to $T_{\text{eff}} = 3 500$ K, $[Z/Z_{\odot}] = -2.5$ and $\log g = 4.5$ is missing in this

scheme (cf. Table 1 and Fig. 5), because we have not been able to obtain the constancy of flux with depth during the computation of this model. There are also a few models which have, in the upper layers, a percentage error that it too large in the flux derivative $dH/d\tau_{\text{Ross}}$, indicating the failure of the condition of the constancy of the flux with depth. These models are marked with a slanted entry in Table 1. In some cases, the problem is due to the overcoming of the temperature limit $T = 2 089$ K of the opacity distribution function tables (ODFs) by the temperatures of the uppermost layers of the model. The corresponding synthetic spectra may be of lower quality.

As an example of the spectra which are electronically retrievable, the spectrum for the full 7650 – 8750 Å interval and $T_{\text{eff}} = 5500$ K, $[Z/Z_{\odot}] = -0.5$, $\log g = 3.0$ parameters is presented in Fig. 1. Remaining Figs. 2–93 will focus on the GAIA 8500 – 8750 Å interval only. The effects caused by changing the temperature, the metallicity and the gravity are illustrated in Figs. 2, 3 and 4 respectively.

2.1. The computed spectra

The synthetic spectra are based on the grids of model atmospheres computed by Castelli (1999) with an updated version of the ATLAS9 code (Kurucz 1993a). These models differ from Kurucz's models only for the convection. They are available at Kurucz's website (<http://cfaku5.harvard.edu>).

Our synthetic spectra follow the $\Delta T_{\text{eff}} = 250$ K step of the grid of available model atmospheres, but only a sub-set of the available surface gravities have been explored. Furthermore, only the microturbulent velocity $\xi = 2$ km s⁻¹ was considered.

Synthetic spectra were computed with the SYNTH code of Kurucz (1993b) at a 500 000 resolving power. They were then degraded to the $\lambda/\Delta\lambda = 20 000$ resolving power of the spectra in Paper I by adopting a Gaussian instrumental profile. No rotational velocity and macroturbulent velocity were assumed in our simulations.

In computing the spectra we adopted the solar abundances given by Pagel (1997), while the model atmospheres (which are based on Kurucz' ODFs), use the Anders & Grevesse (1989) solar abundances. Elements for which the abundances in model atmospheres and synthetic spectra differ are N (-0.08) O (-0.06), F (-0.04), S (+0.09), Ar (-0.06), K (-0.12), Sc (+0.08), Ti (+0.04), Fe (-0.15), Sr (+0.07), Zr (+0.10), La (-0.05), Ce (+0.03). The numbers in parenthesis are the logarithmic differences between the abundances from Anders & Grevesse and Pagel.

Kurucz (1995a) has been the source for the atomic lines, Kurucz (1993b) for the molecular lines of C₂, CN, CO and hydrides (CH, NH, OH, MgH, SiH), and Kurucz (1999) for TiO data. More details about atomic and molecular lines can be found in Kurucz (1995b) and in the

Table 1. The Metallicity-Temperature-Gravity grid mapped by our synthetic spectra. The numbers-in-the-boxes give the corresponding electronic figure where the given triplet of spectra is plotted. The entries in *slanted* characters are the six spectra mentioned in Sect. 2, i.e. those with a too large percentage error in the flux derivative $dH/d\tau_{\text{Ross}}$

[Z/Z _⊙] T log g	[Z/Z _⊙] T log g	[Z/Z _⊙] T log g	[Z/Z _⊙] T log g	[Z/Z _⊙] T log g
05 <i>-2.5 3500 1.0</i> <i>-2.5 3500 2.0</i> <i>-1.5 3500 4.5</i>	06 <i>-1.5 3500 1.0</i> <i>-1.5 3500 2.0</i> <i>-1.5 3500 4.5</i>	07 <i>-0.5 3500 1.0</i> <i>-0.5 3500 2.0</i> <i>-0.5 3500 4.5</i>	08 <i>0.0 3500 1.0</i> <i>0.0 3500 2.0</i> <i>0.0 3500 4.5</i>	09 <i>+0.5 3500 1.0</i> <i>+0.5 3500 2.0</i> <i>+0.5 3500 4.5</i>
10 <i>-2.5 3750 1.0</i> <i>-2.5 3750 2.0</i> <i>-2.5 3750 4.5</i>	11 <i>-1.5 3750 1.0</i> <i>-1.5 3750 2.0</i> <i>-1.5 3750 4.5</i>	12 <i>-0.5 3750 1.0</i> <i>-0.5 3750 2.0</i> <i>-0.5 3750 4.5</i>	13 <i>0.0 3750 1.0</i> <i>0.0 3750 2.0</i> <i>0.0 3750 4.5</i>	14 <i>+0.5 3750 1.0</i> <i>+0.5 3750 2.0</i> <i>+0.5 3750 4.5</i>
15 <i>-2.5 4000 1.0</i> <i>-2.5 4000 2.0</i> <i>-2.5 4000 4.5</i>	16 <i>-1.5 4000 1.0</i> <i>-1.5 4000 2.0</i> <i>-1.5 4000 4.5</i>	17 <i>-0.5 4000 1.0</i> <i>-0.5 4000 2.0</i> <i>-0.5 4000 4.5</i>	18 <i>0.0 4000 1.0</i> <i>0.0 4000 2.0</i> <i>0.0 4000 4.5</i>	19 <i>+0.5 4000 1.0</i> <i>+0.5 4000 2.0</i> <i>+0.5 4000 4.5</i>
20 <i>-2.5 4250 1.0</i> <i>-2.5 4250 2.0</i> <i>-2.5 4250 4.5</i>	21 <i>-1.5 4250 1.0</i> <i>-1.5 4250 2.0</i> <i>-1.5 4250 4.5</i>	22 <i>-0.5 4250 1.0</i> <i>-0.5 4250 2.0</i> <i>-0.5 4250 4.5</i>	23 <i>0.0 4250 1.0</i> <i>0.0 4250 2.0</i> <i>0.0 4250 4.5</i>	24 <i>+0.5 4250 1.0</i> <i>+0.5 4250 2.0</i> <i>+0.5 4250 4.5</i>
25 <i>-2.5 4500 1.0</i> <i>-2.5 4500 2.0</i> <i>-2.5 4500 4.5</i>	26 <i>-1.5 4500 1.0</i> <i>-1.5 4500 2.0</i> <i>-1.5 4500 4.5</i>	27 <i>-0.5 4500 1.0</i> <i>-0.5 4500 2.0</i> <i>-0.5 4500 4.5</i>	28 <i>0.0 4500 1.0</i> <i>0.0 4500 2.0</i> <i>0.0 4500 4.5</i>	29 <i>+0.5 4500 1.0</i> <i>+0.5 4500 2.0</i> <i>+0.5 4500 4.5</i>
30 <i>-2.5 4750 1.0</i> <i>-2.5 4750 2.0</i> <i>-2.5 4750 4.5</i>	31 <i>-1.5 4750 1.0</i> <i>-1.5 4750 2.0</i> <i>-1.5 4750 4.5</i>	32 <i>-0.5 4750 1.0</i> <i>-0.5 4750 2.0</i> <i>-0.5 4750 4.5</i>	33 <i>0.0 4750 1.0</i> <i>0.0 4750 2.0</i> <i>0.0 4750 4.5</i>	34 <i>+0.5 4750 1.0</i> <i>+0.5 4750 2.0</i> <i>+0.5 4750 4.5</i>
35 <i>-2.5 5000 1.0</i> <i>-2.5 5000 2.0</i> <i>-2.5 5000 4.5</i>	36 <i>-1.5 5000 1.0</i> <i>-1.5 5000 2.0</i> <i>-1.5 5000 4.5</i>	37 <i>-0.5 5000 1.0</i> <i>-0.5 5000 2.0</i> <i>-0.5 5000 4.5</i>	38 <i>0.0 5000 1.0</i> <i>0.0 5000 2.0</i> <i>0.0 5000 4.5</i>	39 <i>+0.5 5000 1.0</i> <i>+0.5 5000 2.0</i> <i>+0.5 5000 4.5</i>
40 <i>-2.5 5250 2.0</i> <i>-2.5 5250 3.0</i> <i>-2.5 5250 4.5</i>	41 <i>-1.5 5250 2.0</i> <i>-1.5 5250 3.0</i> <i>-1.5 5250 4.5</i>	42 <i>-0.5 5250 2.0</i> <i>-0.5 5250 3.0</i> <i>-0.5 5250 4.5</i>	43 <i>0.0 5250 2.0</i> <i>0.0 5250 3.0</i> <i>0.0 5250 4.5</i>	44 <i>+0.5 5250 2.0</i> <i>+0.5 5250 3.0</i> <i>+0.5 5250 4.5</i>
45 <i>-2.5 5500 2.0</i> <i>-2.5 5500 3.0</i> <i>-2.5 5500 4.5</i>	46 <i>-1.5 5500 2.0</i> <i>-1.5 5500 3.0</i> <i>-1.5 5500 4.5</i>	47 <i>-0.5 5500 2.0</i> <i>-0.5 5500 3.0</i> <i>-0.5 5500 4.5</i>	48 <i>0.0 5500 2.0</i> <i>0.0 5500 3.0</i> <i>0.0 5500 4.5</i>	49 <i>+0.5 5500 2.0</i> <i>+0.5 5500 3.0</i> <i>+0.5 5500 4.5</i>
50 <i>-2.5 5750 2.0</i> <i>-2.5 5750 3.0</i> <i>-2.5 5750 4.5</i>	51 <i>-1.5 5750 2.0</i> <i>-1.5 5750 3.0</i> <i>-1.5 5750 4.5</i>	52 <i>-0.5 5750 2.0</i> <i>-0.5 5750 3.0</i> <i>-0.5 5750 4.5</i>	53 <i>0.0 5750 2.0</i> <i>0.0 5750 3.0</i> <i>0.0 5750 4.5</i>	54 <i>+0.5 5750 2.0</i> <i>+0.5 5750 3.0</i> <i>+0.5 5750 4.5</i>
55 <i>-2.5 6000 2.0</i> <i>-2.5 6000 3.0</i> <i>-2.5 6000 4.5</i>	56 <i>-1.5 6000 2.0</i> <i>-1.5 6000 3.0</i> <i>-1.5 6000 4.5</i>	57 <i>-0.5 6000 2.0</i> <i>-0.5 6000 3.0</i> <i>-0.5 6000 4.5</i>	58 <i>0.0 6000 2.0</i> <i>0.0 6000 3.0</i> <i>0.0 6000 4.5</i>	59 <i>+0.5 6000 2.0</i> <i>+0.5 6000 3.0</i> <i>+0.5 6000 4.5</i>
60 <i>-2.5 6250 2.0</i> <i>-2.5 6250 3.0</i> <i>-2.5 6250 4.5</i>	61 <i>-1.5 6250 2.0</i> <i>-1.5 6250 3.0</i> <i>-1.5 6250 4.5</i>	62 <i>-0.5 6250 2.0</i> <i>-0.5 6250 3.0</i> <i>-0.5 6250 4.5</i>	63 <i>0.0 6250 2.0</i> <i>0.0 6250 3.0</i> <i>0.0 6250 4.5</i>	64 <i>+0.5 6250 2.0</i> <i>+0.5 6250 3.0</i> <i>+0.5 6250 4.5</i>
65 <i>-2.5 6500 2.0</i> <i>-2.5 6500 3.0</i> <i>-2.5 6500 4.5</i>	66 <i>-1.5 6500 2.0</i> <i>-1.5 6500 3.0</i> <i>-1.5 6500 4.5</i>	67 <i>-0.5 6500 2.0</i> <i>-0.5 6500 3.0</i> <i>-0.5 6500 4.5</i>	68 <i>0.0 6500 2.0</i> <i>0.0 6500 3.0</i> <i>0.0 6500 4.5</i>	69 <i>+0.5 6500 2.0</i> <i>+0.5 6500 3.0</i> <i>+0.5 6500 4.5</i>
70 <i>-2.5 6750 2.0</i> <i>-2.5 6750 3.0</i> <i>-2.5 6750 4.5</i>	71 <i>-1.5 6750 2.0</i> <i>-1.5 6750 3.0</i> <i>-1.5 6750 4.5</i>	72 <i>-0.5 6750 2.0</i> <i>-0.5 6750 3.0</i> <i>-0.5 6750 4.5</i>	73 <i>0.0 6750 2.0</i> <i>0.0 6750 3.0</i> <i>0.0 6750 4.5</i>	74 <i>+0.5 6750 2.0</i> <i>+0.5 6750 3.0</i> <i>+0.5 6750 4.5</i>
75 <i>-2.5 7000 2.0</i> <i>-2.5 7000 3.0</i> <i>-2.5 7000 4.5</i>	76 <i>-1.5 7000 2.0</i> <i>-1.5 7000 3.0</i> <i>-1.5 7000 4.5</i>	77 <i>-0.5 7000 2.0</i> <i>-0.5 7000 3.0</i> <i>-0.5 7000 4.5</i>	78 <i>0.0 7000 2.0</i> <i>0.0 7000 3.0</i> <i>0.0 7000 4.5</i>	79 <i>+0.5 7000 2.0</i> <i>+0.5 7000 3.0</i> <i>+0.5 7000 4.5</i>
80 <i>-2.5 7250 2.0</i> <i>-2.5 7250 3.0</i> <i>-2.5 7250 4.5</i>	81 <i>-1.5 7250 2.0</i> <i>-1.5 7250 3.0</i> <i>-1.5 7250 4.5</i>	82 <i>-0.5 7250 2.0</i> <i>-0.5 7250 3.0</i> <i>-0.5 7250 4.5</i>	83 <i>0.0 7250 2.0</i> <i>0.0 7250 3.0</i> <i>0.0 7250 4.5</i>	84 <i>+0.5 7250 2.0</i> <i>+0.5 7250 3.0</i> <i>+0.5 7250 4.5</i>
85 <i>-2.5 7500 2.0</i> <i>-2.5 7500 3.0</i> <i>-2.5 7500 4.5</i>	86 <i>-1.5 7500 2.0</i> <i>-1.5 7500 3.0</i> <i>-1.5 7500 4.5</i>	87 <i>-0.5 7500 2.0</i> <i>-0.5 7500 3.0</i> <i>-0.5 7500 4.5</i>	88 <i>0.0 7500 2.0</i> <i>0.0 7500 3.0</i> <i>0.0 7500 4.5</i>	89 <i>+0.5 7500 2.0</i> <i>+0.5 7500 3.0</i> <i>+0.5 7500 4.5</i>

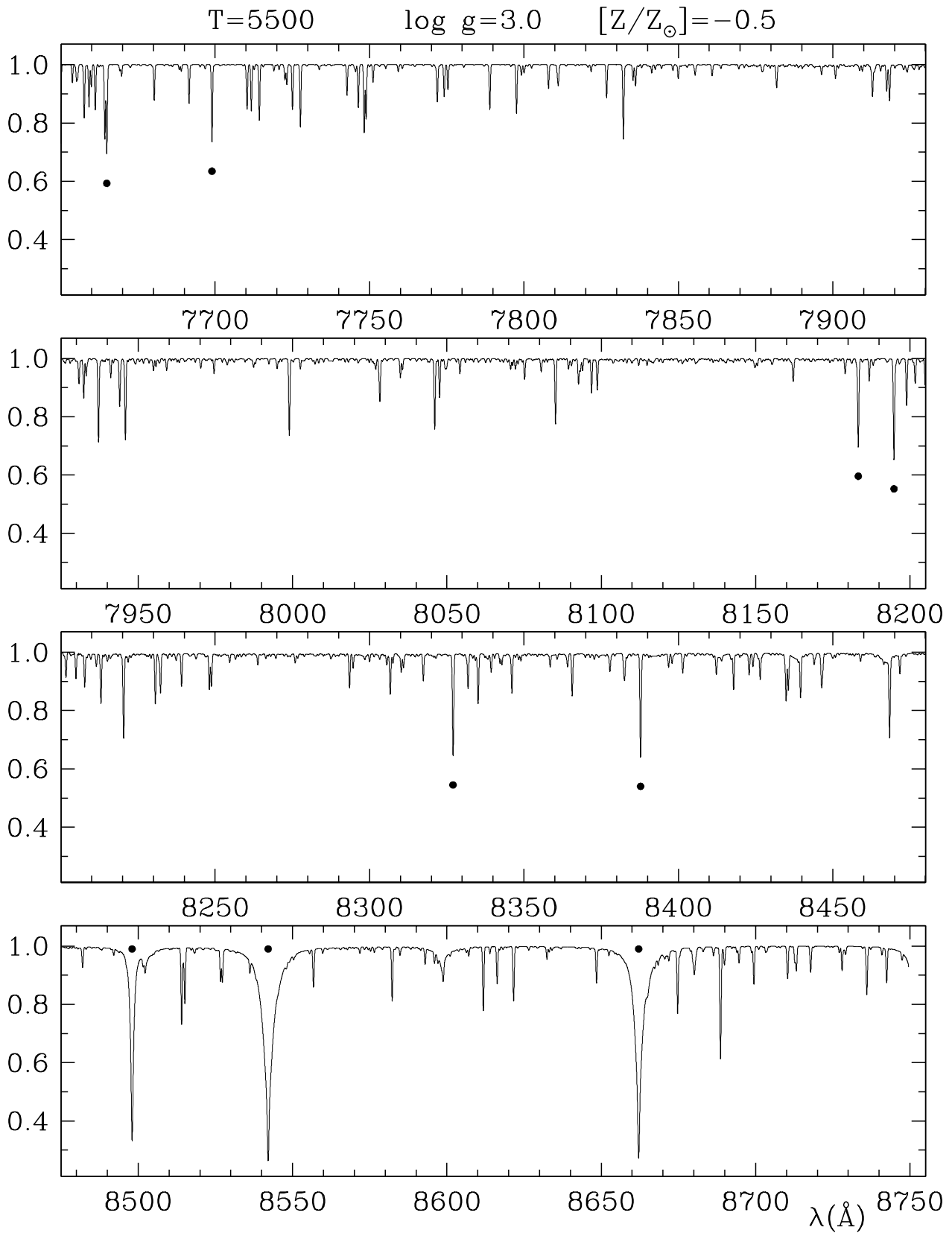


Fig. 1. All spectra have been computed over a range wider than the 8500 – 8750 Å considered in this series of papers. This plot shows the full explored range (7650 – 8750 Å). The filled circles point to the K I, Na I, Fe I and Ca II lines discussed in Sect. 1

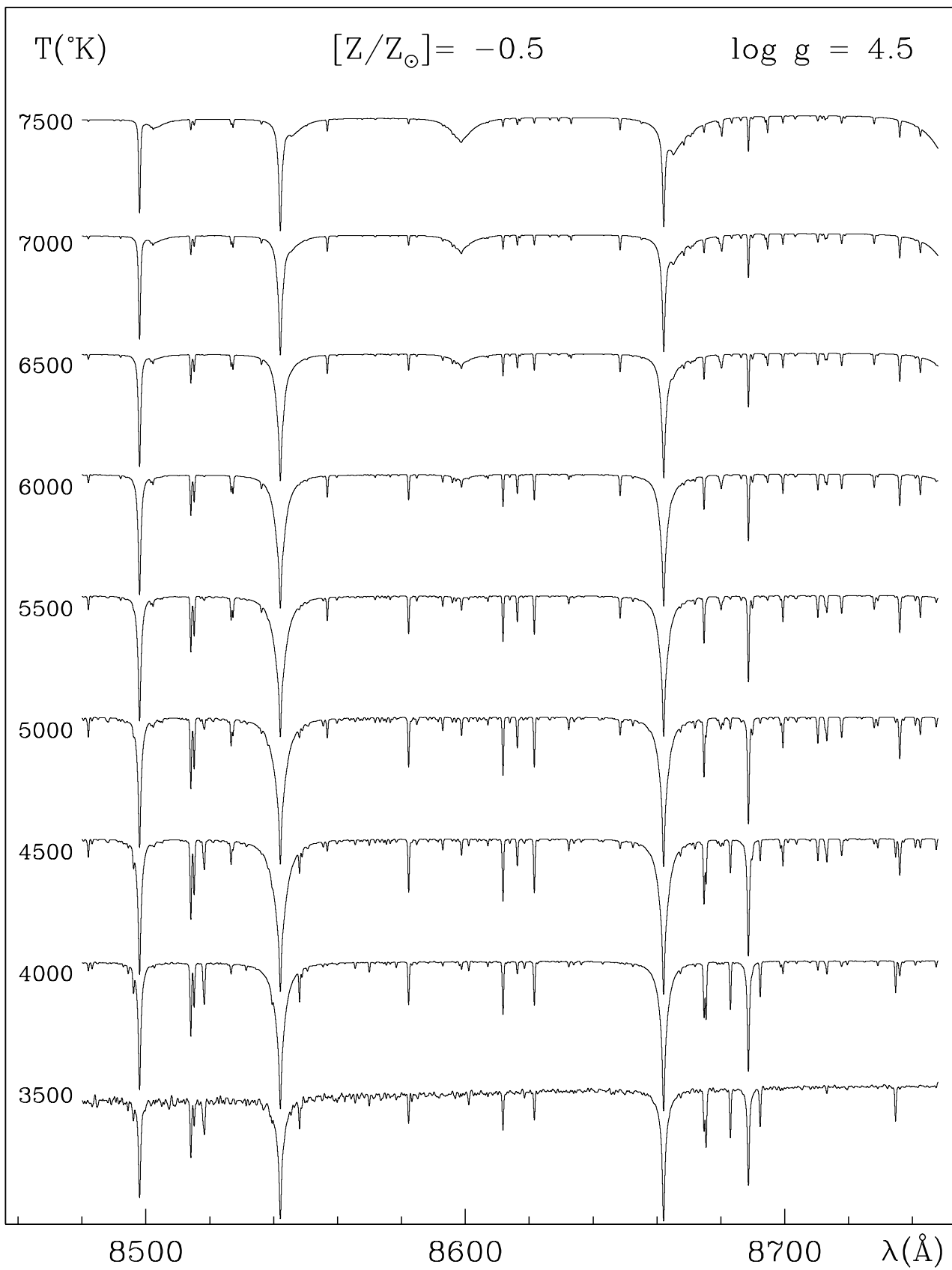


Fig. 2. A sample of $[Z/Z_{\odot}] = -0.5$, $\log g = 4.5$ synthetic spectra arranged in a sequence showing the effect of varying the temperature

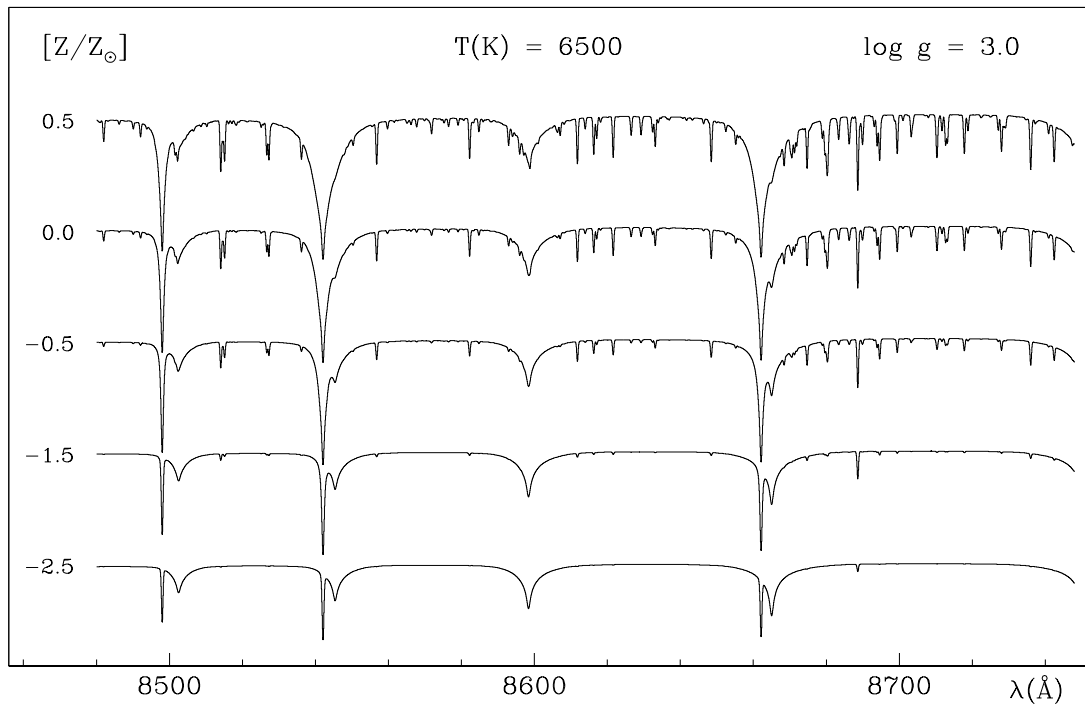


Fig. 3. A sample of $T_{\text{eff}} = 6500$ K, $\log g = 3.0$ synthetic spectra arranged in a sequence showing the effect of varying the metallicity

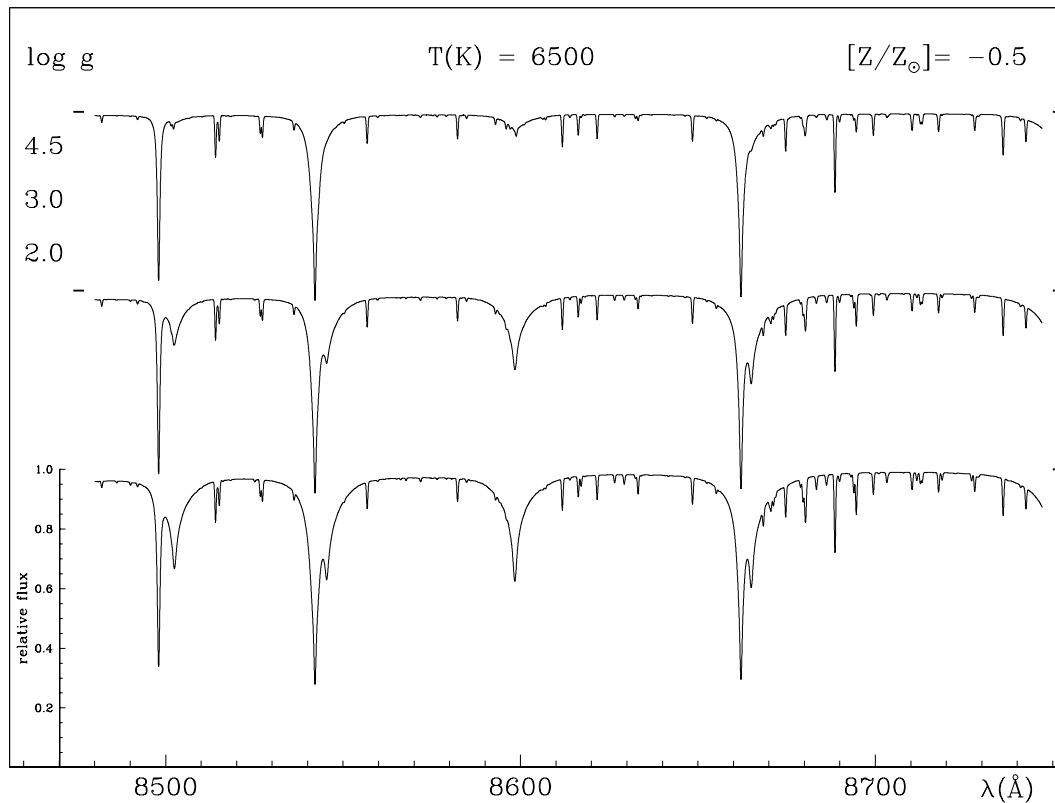


Fig. 4. A sample of $T_{\text{eff}} = 6500$ K, $[Z/Z_{\odot}] = -0.5$ synthetic spectra arranged in a sequence showing the effect of varying the gravity. The thick dashes mark the 1.00 level of the continuum. This is an example of the Figs. 5–89 only available electronically

Kurucz website. Molecular lines were considered for the models with $T_{\text{eff}} \leq 6500$ K. The TiO contribution is inessential at all temperatures for $[Z/Z_{\odot}] = -2.5$, while it becomes significant at $T_{\text{eff}} = 3750$ K for $[Z/Z_{\odot}] = -1.5$, $T_{\text{eff}} = 4000$ K for $[Z/Z_{\odot}] = -0.5$, $T_{\text{eff}} = 4250$ K for $[Z/Z_{\odot}] = 0.0$, and $T_{\text{eff}} = 4500$ K for $[Z/Z_{\odot}] = +0.5$. The CN is the molecule with the strongest lines in the GAIA 8500 – 8750 Å region for the models with $T_{\text{eff}} \geq 4500$ K.

To assess the usefulness of the computed spectra we compare three of them with real spectra in Figs. 90, 91 and 92. Figure 90 shows the comparison between the $T_{\text{eff}} = 5750$ K, $[Z/Z_{\odot}] = 0.0$, $\log g = 4.5$ synthetic spectrum and the Sun observed spectrum taken from Kurucz et al. (1984) atlas (degraded to 20 000 resolving power). Figures 91 and 92 compare the observed spectra for G5 V and K5 V stars from Paper I with the closest synthetic spectra here computed.

In the comparison against the Sun, the larger wings for the Ca II lines are mostly related to the structure of the ATLAS9 models. When the Holweger-Müller (1974) solar empirical model is used the agreement with the observed spectrum improves considerably. The same effect was shown by Cayrel et al. (1996) for the solar Ca I triplet at 6102, 6122, and 6162 Å. About the comparison with stars other than our Sun, the reader should bear in mind that our spectra are not intended to match any star in particular (which will have non zero rotational and macroturbulent velocities, a microturbulent velocity probably different from the $\xi = 2$ km s⁻¹ here adopted, and a quite probable non-solar partition of the metal abundances). The present atlas instead is intended to explore the effects of changing the basic parameters describing the spectrum of a star in order to provide the simulations of GAIA observations with a realistic and complete set of input spectra.

The comparisons in Figs. 90–92 indicate that the synthetic spectra well represent the real spectra. They therefore constitute a useful input databank for simulations of GAIA observations as well as an aid to ground-observer spectroscopists working at moderately high resolving power ($\lambda/\Delta\lambda \sim 10^4$) in the near-IR region of the spectrum. The original computation at a 500 000 resolving power will allow us to re-map the whole grid of synthetic spectra at any resolution that the industrial designing of GAIA should require other than the currently baselined $\lambda/\Delta\lambda = 20\,000$.

The interested reader can evaluate the effects of changing the microturbulent velocity ξ by inspecting Fig. 93 where a zoomed portion of three spectra with the same $T_{\text{eff}} = 5750$ K, $\log g = 2.0$ and $[Z/Z_{\odot}] = 0.0$ but different microturbulent velocities ($\xi = 1, 2$ and 4 km s⁻¹) are compared. The comparison is intentionally carried out for a gravity typical of a supergiant because the effect of the microturbulent velocity increases with decreasing gravity.

2.2. The atlas

The 254 spectra are presented in Figs. 5 to 89 (available only electronically) following the scheme in Table 1. Each figure is devoted to a triplet of spectra characterized by the same temperature and metallicity but with different surface gravities. This arrangement is quite similar to that of Paper I where the spectra were arranged into luminosity sequences at a given spectral type, and should facilitate the intercomparison between observed and synthetic spectra.

Only the 8490 – 8750 Å interval of interest to the baseline configuration of GAIA is presented in the figures. The remaining 7650 – 8490 Å interval is available only via the spectra in electronic form. The most relevant lines in the 8490 – 8750 Å range are tabulated in Table 2.

3. The performance of the 8500 – 8750 Å region in the GAIA context

The principal reason to have a spectrograph of suitable resolution aboard the GAIA astrometric mission is to provide the 6th component of the phase-space coordinates. GAIA will observe in scanning-mode, therefore all targets will be observed for the same exposure time irrespective of their magnitude. Given the brightness population index for field stars (an increase of 1 in the limiting magnitude roughly triples the number of stars), the vast majority of GAIA targets will be found among the stars providing the weakest signal above a given threshold.

The weaker the spectrum, the stronger must be the spectral features to maintain a reasonable accuracy in the radial velocities (cf. M 99). The grid of spectra presented in this paper show how in the whole near-IR region explored (7650 – 8750 Å), the Ca II triplet is by far the strongest feature for the spectral types, luminosity classes and metal abundances accounting for the vast majority of the GAIA targets.

Therefore, the present atlas adds support to the superior performance of the 8500 – 8750 Å region in meeting the GAIA demands on radial velocities (cf. M 99 for a discussion about the performances in terms of rotational velocities, spectral classification, chemical abundances, detection of mass loss and peculiarities, signatures of interstellar reddening).

References

- Anders E., Grevesse N., 1989, *Geochim. Cosmochim. Acta* 53, 197
- Black J.H., Wisheit J.C., Laviana E., 1972, *ApJ* 177, 567
- Castelli F., 1999, *A&A* 346, 564
- Cayrel R., Faurobert-Scholl M., Feautrier A., Spielfieldel A., Th́venin F., 1996, *A&A* 312, 549

- Figger H., Heldt J., Siomos K., Walther H., 1975, *A&A* 43, 389
- Fuhr J.R., Martin G.A., Wiese W.L., 1988, *J. Phys. Chem. Ref. Data* 17, Suppl. 4
- Gilmore G., Perryman M., Lindegren L., et al., 1998, *Proc. SPIE Conf.* 3350, 541
- Holweger H., Müller E.A., 1974, *Solar Phys.* 39, 19
- Kurucz R.L., 1988, *Trans. IAU, XXB*, McNally M. (ed.). Kluwer, p. 168
- Kurucz R.L., 1993a, *ATLAS9 Stellar Atmospheres Programs and 2 km s⁻¹ grid*, CD-ROM No. 13
- Kurucz R.L., 1993b, *SYNTH3 Spectrum Synthesis Programs and Line Data*, CD-ROM No. 18
- Kurucz R.L., 1995a, *Atomic Line List*, CD-ROM No. 23
- Kurucz R.L., 1995b, *Astrophysical Applications of Powerful New Databases*, Adelman S.J. & Wiese W.L. (eds.), *ASP Conf.* 78, 205
- Kurucz R.L., Peytremann E., 1975, *SAO Special Report* 362
- Kurucz R.L., Furenlid I., Brault J., Testerman L., 1984, *Solar Flux Atlas from 296 to 1300 nm*, National Solar Obs., Sunspot, p. 240
- Kurucz R.L., 1999, *TiO Linelist from Schwenke (1998) CD-ROM* 24
- Lambert D.L., 1968, *MNRAS* 138, 143
- Martin G.A., Fuhr J.R., Wiese W.L., 1988, *J. Phys. Chem. Ref. Data* 17, Suppl. 3
- Merat P., Safa F., Camus J.P., Pace O., Perryman M.A.C., 1999, in: *Proceedings of the ESA Leiden Workshop on GAIA*, 23-27 Nov. 1998, *Baltic Astron.* 8, 1
- Munari U., 1999, in: *Proceedings of the ESA Leiden Workshop on GAIA*, 23-27 Nov. 1998, *Baltic Astron.* 8, 73 (M 99)
- Munari U., Tomasella L., 1999, *A&AS* 137, 521 (Paper I)
- Pagel B.E.J., 1997, *Nucleosynthesis and Chemical Evolution of Galaxies*. Cambridge University Press, p. 84
- Wiese W.L., Smith M.W., Glennon B.M., 1966, *NSRDS-NBS* 4